



NAZARBAYEV  
UNIVERSITY

School of Engineering and Digital Sciences

Mechanical and Aerospace Engineering, Bachelor of Engineering

# **Design and Optimization of Regenerative Braking System**

By

Zhalelov Batyrlan

Rustem Tnymkulov

Yernur Sailaubek

Nurbek Turaly

Supervisor: Desmond Adair

April, 2024

## DECLARATION

We, Zhalelov Batyrlan, Rustem Tnymkulov, Yernur Sailaubek, and Nurbek Turaly hereby declare that this report, entitled “Design and Optimization of Regenerative Braking System,” is the result of our own project work except for quotations and citations which have been duly acknowledged. We also declare that it has not been previously or concurrently submitted for any other degree at Nazarbayev University or elsewhere.

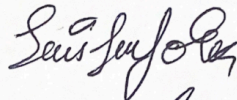
Name: Zhalelov Batyrlan



Name: Rustem Tnymkulov



Name: Yernur Sailaubek



Name: Nurbek Turaly



Date: 28.04.2024

## **ABSTRACT**

The research was conducted to explore a unique modern method of recuperation called the regenerative braking system. The concept behind that is to generate voltage from the source of heat. The device that was used in our case is a Thermoelectric generator(TEG). This device converts the temperature difference into the potential difference.

As the braking is performed, there is an enormous amount of energy that is just dissipated in the rotor, and released to the environment. The study explores the way to implement the TEG into the braking system, find the best possible assembling approach, and discover whether the output parameters are going to be sufficient for the implementation of helpful systems.

In order to achieve the aims that were set, simulations, as well as hand calculations were applied. Results were obtained by using different softwares such as ANSYS, Solidworks, MATLAB and Excel. From the presented data, the analysis of the selected design was executed. Figuring out the applications that can be theoretically implemented with the help of regenerative braking systems, as well as the conditions in which they are the most effective

## **ACKNOWLEDGMENTS**

We would like to express our special thanks to adviser Desmond Adair for his big help in our capstone project provided throughout the year. Your advice and opinion was important and significant for our capstone project.

## TABLE OF CONTENTS

<b>ABSTRACT.....</b>	<b>2</b>
<b>LIST OF FIGURES.....</b>	<b>5</b>
<b>LIST OF TABLES.....</b>	<b>6</b>
<b>LIST OF ABBREVIATIONS, NOTATIONS / GLOSSARY OF TERMS.....</b>	<b>7</b>
<b>1. INTRODUCTION.....</b>	<b>1</b>
<b>2. LITERATURE REVIEW.....</b>	<b>1</b>
2.1 Braking energy dissipation.....	1
2.2 Thermoelectricity.....	2
2.3 The Seebeck effect.....	3
2.4 Thermoelectric generator.....	4
2.5 Performance parameters of TEG.....	4
2.6 Proposed wiring solution.....	6
<b>3. METHODOLOGY.....</b>	<b>8</b>
3.1 Modeling of brake disk.....	8
3.2 Modeling of TEG.....	10
3.3 Braking energy dissipation.....	12
<b>4. RESULTS AND DISCUSSION.....</b>	<b>16</b>
4.1. Ansys results.....	16
4.2. The TEG module’s parameters calculations.....	22
4.3. Our team’s proposed design.....	26
<b>5. CONCLUSION.....</b>	<b>29</b>
<b>REFERENCES.....</b>	<b>30</b>
<b>APPENDICES.....</b>	<b>32</b>

## LIST OF FIGURES

- Figure 1. Thermoelectric module*
- Figure 2. SR012 Low Voltage Slip Ring Separates by Rotary Systems*
- Figure 3. Proposed design of wiring*
- Figure 4. Disk brake 121.44146 drawing*
- Figure 5. Right view of brake disk*
- Figure 6. Isometric view of brake disk*
- Figure 7. TEG modules inside the brake disk*
- Figure 8. P-type and N-type legs layout view*
- Figure 9. Simplified TEG module for simulation*
- Figure 10. Meshing of brake disk*
- Figure 11. Mesh for the TEG*
- Figure 12. Front side temperature distribution for 40km/h*
- Figure 13. Back side temperature distribution for braking from 40 km/h.*
- Figure 14. Front side temperature distribution for braking from 60 km/h*
- Figure 15. Back side temperature distribution for braking from 60 km/h*
- Figure 16. Front side temperature distribution for braking from 80 km/h*
- Figure 17. Back side temperature distribution for braking from 80 km/h*
- Figure 18. Results for the total current density.*
- Figure 19. Thermal analysis of a TEG.*
- Figure 20. Thermal efficiency against resistive load graph*
- Figure 21. Electrical current against resistive load graph*
- Figure 22. Voltage against resistive load graph*
- Figure 23. Power output against resistive load graph*
- Figure 24. The design of the TEGs connection with the slip ring with wirings*
- Figure 25. Side view of the TEGs connection with the slip ring with wirings*
- Figure 26. Exploded view of the TEGs connection with the slip ring with wirings*

## **LIST OF TABLES**

*Table 1. Brake disk specification*

*Table 2. Properties of cast iron*

*Table 3. Dimensions and physical properties of TEG*

*Table 4. Braking power and heat flux for different scenarios*

*Table 6. Maximum parameters of single TEG at different temperatures*

## LIST OF ABBREVIATIONS, NOTATIONS / GLOSSARY OF TERMS

*TEG* Thermoelectric generator

*Z* Figure of merit

$\alpha$  Seebeck coefficient (P-positive and N-negative)

$\rho$  electrical resistivity

*k* thermal conductivity

$Q_h$  heat absorbed at hot junction

$T_h$  temperature at hot junction

$T_c$  temperature at cold junction

$\bar{T}$  absolute temperature

*R* electrical resistance

$R_L$  external load resistance

*K* thermal conductance

*L* length of the semiconductor (N-type and P-type)

*A* cross-sectional area of the semiconductor

$A_{disk}$  braking section area

*I* electrical current

$I_{max}$  maximum current

$V_n$  voltage

$V_{max}$  maximum voltage

$W_n$  power output



$W_{max}$  maximum power output

$\eta_{th}$  thermal efficiency

$\eta_{max}$  maximum thermal efficiency

$\eta_{mp}$  maximum power efficiency

$E_L$  energy loss

$g$  acceleration due to gravity

$f$  friction factor with road

$\lambda$  braking efficiency distribution

$P$  braking power

$q$  heat flux

$s$  stopping distance

$t$  stopping time

$\vartheta_0$  initial speed

$\vartheta_f$  final speed

$m$  mass of car

$d_{outer}$  outer diameter of brake disk

$d_{inner}$  inner diameter of brake disk

## **1. INTRODUCTION**

Nowadays, the problem of insufficient energy waste is becoming as relevant as ever. With the small amount of devices that use green energy, energy waste is an issue that is critical for both economical and environmental reasons. Vehicle efficiency is a feature that was developed long ago, and with all today's advancements it is still an issue that has many ways to improve. The amount of energy that is dissipated in the braking system while performing braking is enormous, which we regard as an opportunity to improve its efficiency.

One way to improve a vehicle's efficiency, a Regenerative braking system, is presented in this project. The energy that is dissipated in a brake rotor can be absorbed by a Thermoelectric Generator(TEG). This form of recuperation requires a temperature difference in order to produce a potential difference. This is a modern, environmentally friendly concept, in which electrical power can be used to implement some of the additional devices onto the vehicles such as more advanced control systems, lighting devices, battery charging etc.

The main objectives of the project are to find the best way to implement a regenerative braking system to the urban vehicle, as well as to explore the output parameters. The goal is to find the implementation that satisfies the aims of implementing an electric system, and to recharge the battery of the vehicle.

## **2. LITERATURE REVIEW**

### **2.1 Braking energy dissipation**

The friction between the surfaces of the brake disk and pads produces waste thermal energy during the braking period of the vehicle. Then, this heat energy is dissipated into the medium. The energy is then stored in the rotor in the form of heat and can reach a high

temperature of around 200 degrees Celsius. This energy that is already stored as an increased temperature can be absorbed with the TEG.

The regeneration of the lost thermal energy significantly depends on the temperature of the system and the material subject to friction. Therefore, it is crucial that the temperature of the heat source is bigger than the heat sink temperature or ambient temperature of the environment in our case. The difference between the heat source and sink temperatures plays an important role in determining the power generated by the thermoelectric generator. According to Coulibaly et al. (2021), a ventilated brake disk reaches around 176 °C at an initial speed of 60 kilometers per hour, braking time of 3.4 seconds and weight of the vehicle of 1425 kilograms [1]. In the paper, that energy corresponds to a heat flux of around  $900000 \text{ W/m}^2$ . This is a great opportunity to perform recuperation and the studies on which have to be conducted. According to the study of Coulibaly, an estimated thermoelectric generator produced around 3.25 Watts, which proves that energy recovery is possible in the braking system of the vehicles.

The energy and power loss during braking can be determined by determining the kinetic energy of the vehicle. The first law of thermodynamics states the energy conservation within the system, where kinetic energy transfers to the heat energy. It is important to highlight the fact that the braking efficiency distribution on the front and back wheels is not equal, where the front wheels exert 60% and the back wheels exert 40% [1].

## **2.2 Thermoelectricity**

The process of converting energy from thermal into electrical energy is called thermoelectricity. The conversion of energy is possible in the opposite direction, from electrical into thermal. The electrical flow is generated when a different temperature is applied to opposite sides of the thermoelectric device. Similarly, applying a voltage to these devices causes a

temperature difference. A temperature difference makes charge carriers in the material diffuse from the hot side to the cold side, generating current flow. This effect has the potential to generate power, measure temperature, and change the temperature of objects. The thermoelectric effect includes the Seebeck effect and the Peltier effect. We will consider the Seebeck effect only as we are interested in converting thermal energy into electrical energy. This section discusses thermoelectric effects.

### 2.3 The Seebeck effect

This is the effect that allows thermoelectric generators to generate power. It is the direct conversion of temperature differences into electricity. Seebeck found in 1821 that if there was a temperature differential between the junctions, a compass needle was deflected by a closed loop produced by two metals linked in two places. This is due to the fact that metals react differently to temperature differences, resulting in a current loop and a magnetic field. Seebeck never recognized the presence of an electric current, but Hans Christian Oersted eventually corrected the error and developed the term thermoelectricity. The created voltage can be calculated by the next formula:

$$V = \int_{T_1}^{T_2} [\alpha_p(T) - \alpha_N(T)] dT \quad (1)$$

where  $\alpha_p$  is P-type material's Seebeck coefficient,  $\alpha_N$  is N-type material's Seebeck coefficient and  $T_1$  and  $T_2$  - temperatures of the two junctions.

The Seebeck coefficients are functions of temperature. Material parameters are the other factor that affects the seebeck coefficient. The positive sign of the seebeck coefficient means that the emf tends to drive the current from the hot to cold junction. If the opposite signs are used the emf is added.

## 2.4 Thermoelectric generator

The device that uses the Seebeck effect and converts thermal energy into electrical energy is the thermoelectric generator. It consists of p and n types of semiconductors which are connected in series electrically and in parallel thermally. They are placed between two plates which are good heat conductors but at the same time electrical insulators. One side of the plate is subjected to high temperature while the second side must be cold, thus creating the temperature difference between two sides of semiconductors.

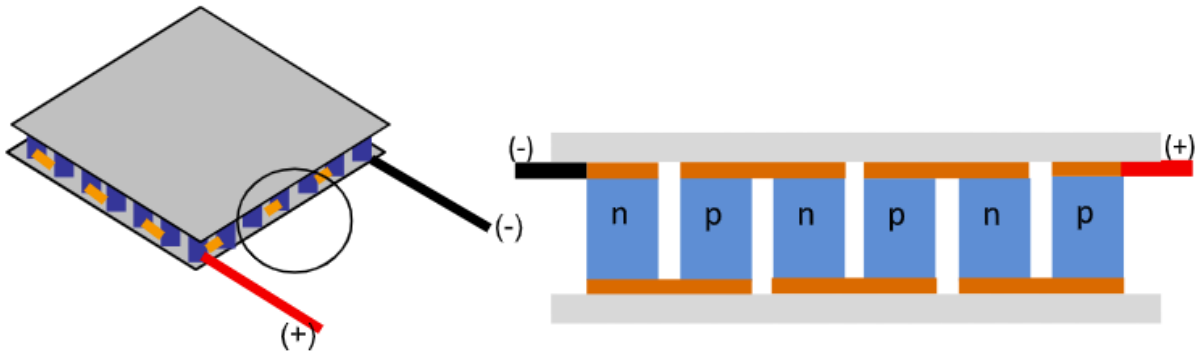


Figure 1. Thermoelectric module [3]

## 2.5 Performance parameters of TEG

The figure of merit ( $Z$ ) is a measure of performance of TEG, with units of  $1/K$ .

$$Z = \frac{\alpha^2}{\rho k} \quad (2)$$

where  $\alpha$  is the Seebeck coefficient,  $\rho$  is the electrical resistivity and  $k$  is the thermal conductivity.

The dimensionless figure of merit is product of figure of merit and absolute temperature ( $\bar{T}$ ). Absolute temperature equals the arithmetic mean of temperatures on hot and cold junctions. In the Thermoelectrics book written by HoSung Lee, it states that the energy conversion efficiency of the material increases with the greater value of the dimensionless figure of merit

[2]. The power factor of the TEG is defined by  $\alpha^2/\rho$ . Therefore, the Seebeck coefficient must be large, while the electrical resistivity and thermal conductivity must be small.

The heat absorption rate value ( $Q_h$ ) at the hot junction is shown in Formula 3 [2].

$$Q_h = n \left[ \alpha T_h I - \frac{1}{2} I^2 R + K(T_h - T_c) \right] \quad (3)$$

where

$$\alpha = \alpha_p - \alpha_n \quad (4)$$

$$R = \frac{\rho_p L_p}{A_p} + \frac{\rho_n L_n}{A_n} \quad (5)$$

$$K = \frac{k_p A_p}{L_p} + \frac{k_n A_n}{L_n} \quad (6)$$

where  $T_h$  is the temperature at hot junction,  $T_c$  is the temperature at cold junction,  $R$  is the electrical resistance,  $K$  is the thermal conductance,  $L$  is the length of the semiconductor (N-type and P-type),  $A$  is the cross-sectional area of the semiconductor.

The current of the module ( $I$ ) is independent of the thermocouples quantity and is expressed as [2]

$$I = \frac{\alpha(T_h - T_c)}{R_L + R} \quad (7)$$

where  $I$  is the electrical current,  $R_L$  is the external load resistance.

The voltage across the module ( $V_n$ ) is expressed as

$$V_n = \frac{n\alpha(T_h - T_c)}{R_L/R + 1} \left( \frac{R_L}{R} \right) \quad (8)$$

The output power of the module ( $W_n$ ) is shown below as follows.

$$W_n = \frac{n\alpha^2(T_h - T_c)^2}{R} \frac{R_L/R}{(1 + R_L/R)^2} \quad (9)$$

The ratio of the output power to heat absorbed at the hot junction is equal to the thermal efficiency ( $\eta_{th}$ ).

$$\eta_{th} = \frac{W_n}{Q_h} \quad (10)$$

The maximum parameters of TEG can be found using Formulas from 7 to 10. The maximum current happens at  $R_L = 0$ . The maximum voltage accordingly at  $I = 0$ . In contrast, the maximum power output occurs at  $R_L/R = 1$  [2].

$$I_{max} = \frac{\alpha(T_h - T_c)}{R} \quad (11)$$

$$V_{max} = n\alpha(T_h - T_c) \quad (12)$$

$$W_{max} = \frac{n\alpha^2(T_h - T_c)^2}{R} \quad (13)$$

It should be noted that there are two efficiencies of the module. First, the maximum thermal efficiency ( $\eta_{max}$ ) occurs at  $R_L/R = \sqrt{1 + Z\bar{T}}$ . Second, The maximum power efficiency ( $\eta_{mp}$ ) occurs at  $R_L/R = 1$  [2].

$$\eta_{max} = \left(1 - \frac{T_c}{T_h}\right) \frac{\sqrt{1+Z\bar{T}}-1}{\sqrt{1+Z\bar{T}}+T_c/T_h} \quad (14)$$

$$\eta_{mp} = \frac{(1-T_c/T_h)}{2 - \frac{1}{2}(1-T_c/T_h) + \frac{2}{Z\bar{T}}(1+T_c/T_h)} \quad (15)$$

These formulas were used later for calculations.

## 2.6 Proposed wiring solution

In this research a serious problem was connected with wirings. As our TEGs are located on a rotating element, the problem of wiring from a rotating part to a fixed part of the car had to be solved. A conceptual solution of the wiring problem was firstly shown by Jie (2015). He

suggested using the conductive ring, a device which allows a continuous transmission of electricity between rotating and fixed parts.

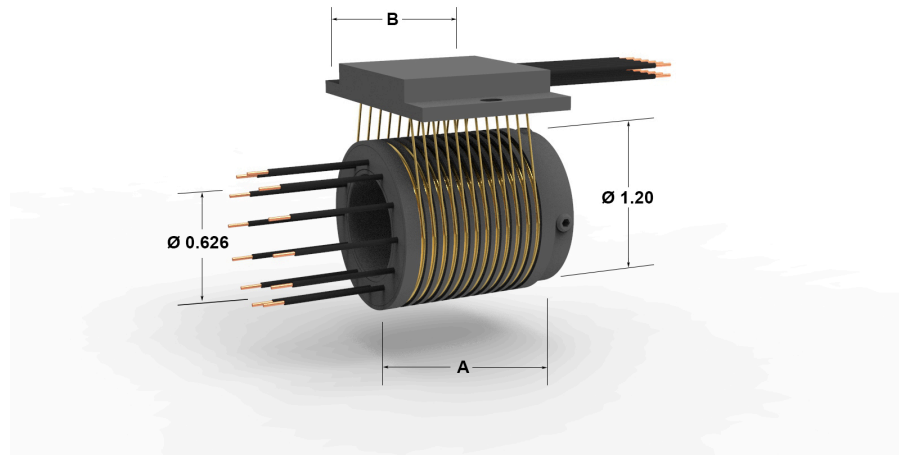


*Figure 2. SR012 Low Voltage Slip Ring Separates by Rotary Systems [4]*

The working principle of the slip ring is simple. It involves a stator (stationary element) and rotor (rotating element). The stator element should be attached to the stationary structure, while the rotor is installed on the shaft. There are conductive rings on the rotor, which is usually made of copper or silver. The rotor with its rings must be mated concentrically around the axis of the shaft. The stator has the brushes which are in constant contact with the rings of the rotor. This constant contact is achievable due to springs which load the brushes. Such construction allows electric flow to be transferred between the stator and rotor without interruption. The slip rings show high performance in terms of loss of energy [5].

The scheme of a conceptual construction of the car system with integrated TEGs and conductive ring is shown below.



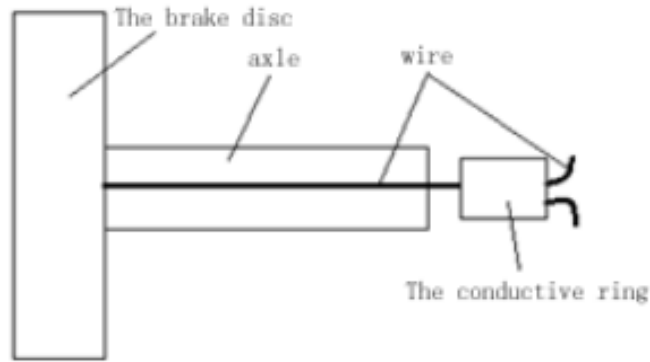


Figure 3. Proposed design of wiring [6].

### 3. METHODOLOGY

#### 3.1 Modeling of brake disk

The brake disk was developed using the SolidWorks application. Toyota Camry was chosen as a test vehicle. The prototype was a real disk of this car made of cast iron for models produced between 2007 and 2017 by the company in Figure 3 [7].

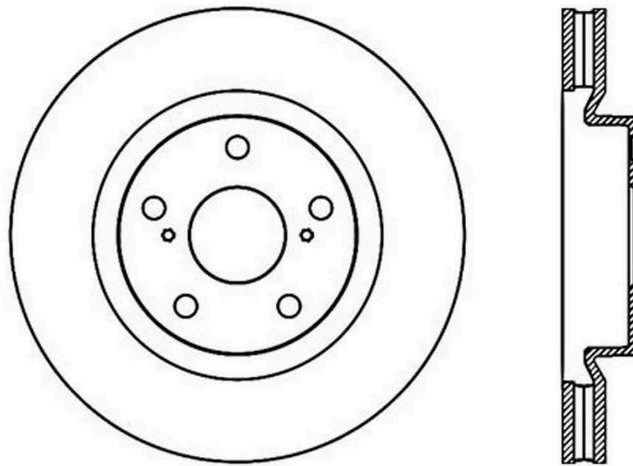
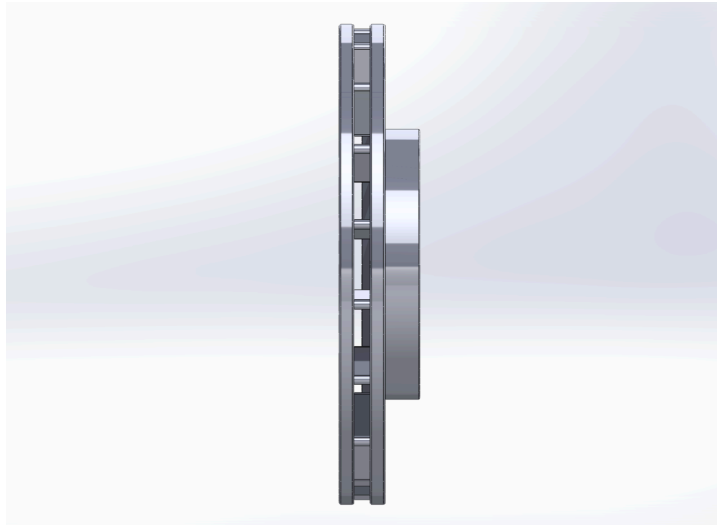


Figure 4. Disk brake 121.44146 drawing [7]

*Table 1. Brake disk specification [7]*

<b>Parameter</b>	Outer diameter	Inner diameter	Height	Thickness	Hub hole diameter	Bolt hole diameter	Bolt circle diameter	Weight
<b>Unit</b>	mm	mm	mm	mm	mm	mm	mm	kg
<b>Value</b>	296	202	49.5	28	62	14.5	114.3	7.5

The table above shows the specifications of the brake disk [7]. The model was developed using exact numbers in Figures 4 and 5 and will be used along with the properties of material in Table 2 later in simulations.



*Figure 5. Right view of brake disk*

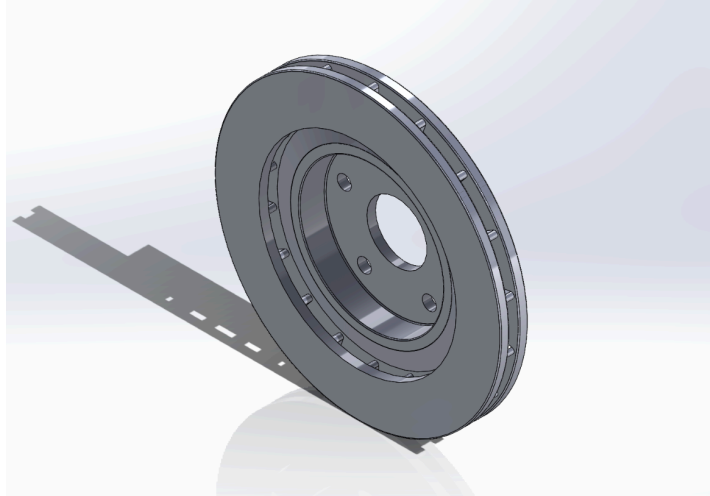


Figure 6. Isometric view of brake disk

Table 2. Properties of cast iron [8]

Property	Unit	Value
Density	$\frac{kg}{m^3}$	7200
Young Modulus	GPa	125
Thermal conductivity	$\frac{W}{m \times K}$	54.5
Specific heat	$\frac{J}{kg \times K}$	586

### 3.2 Modeling of TEG

The TEG was developed using the SolidWorks application. An existing TEG module was selected for the project [9]. This module has high seebeck coefficients which shows good efficiency of material in Table 3. In Figures 7, 8 and 8, the TEG modules in brake disk, its P-type and N-type legs layout schematic view and its simplified module for ANSYS Workbench. As a result, trapezoidal shaped TEG was developed and 156 couples can be fitted inside one module made of Bismuth Telluride ( $Bi_2Te_3$ ). This material is frequently used in TEGs and its best

performance values ( $z\bar{T}$ ) go up 1.5 [12]. The maximum working temperature is approximately 300 °C. TEG modules are connected in series with each other.

*Table 3. Dimensions and physical properties of TEG [9]*

Parameter	Unit	Value
$A$	$m^2$	$1.3 \times 1.3 \times 10^{-6}$
$L$	$m$	$1.5 \times 10^{-3}$
$\alpha_P$	$V/K$	$223.2 \times 10^{-6}$
$\alpha_N$	$V/K$	$-187.7 \times 10^{-6}$
$\rho_P$	$\Omega \times m$	$1.83 \times 10^{-5}$
$\rho_N$	$\Omega \times m$	$1.53 \times 10^{-5}$
$k_P$	$\frac{W}{m \times K}$	1.68
$k_N$	$\frac{W}{m \times K}$	1.64

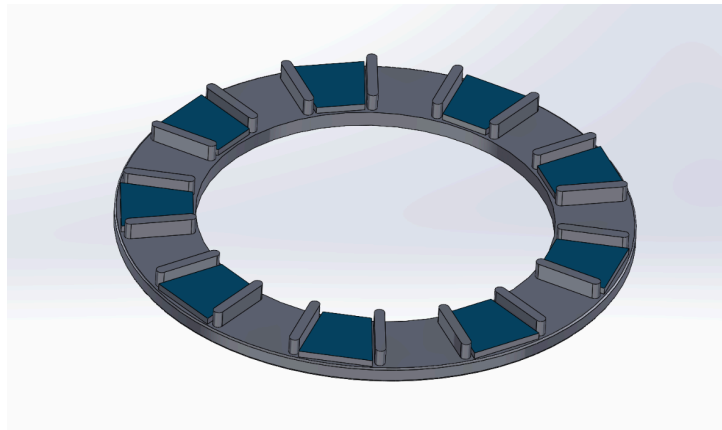


*Figure 7. TEG modules inside the brake disk*

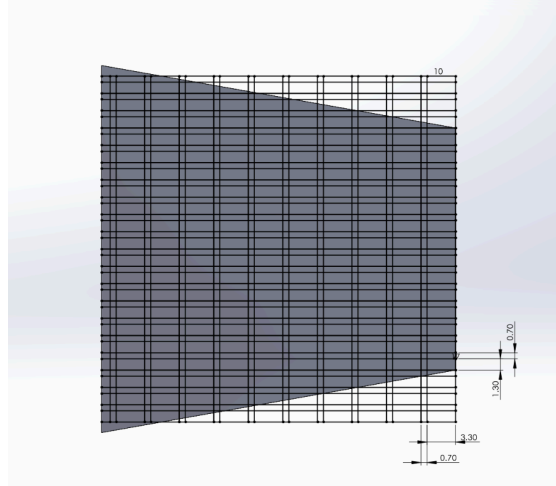


*Figure 8. P-type and N-type legs layout view*

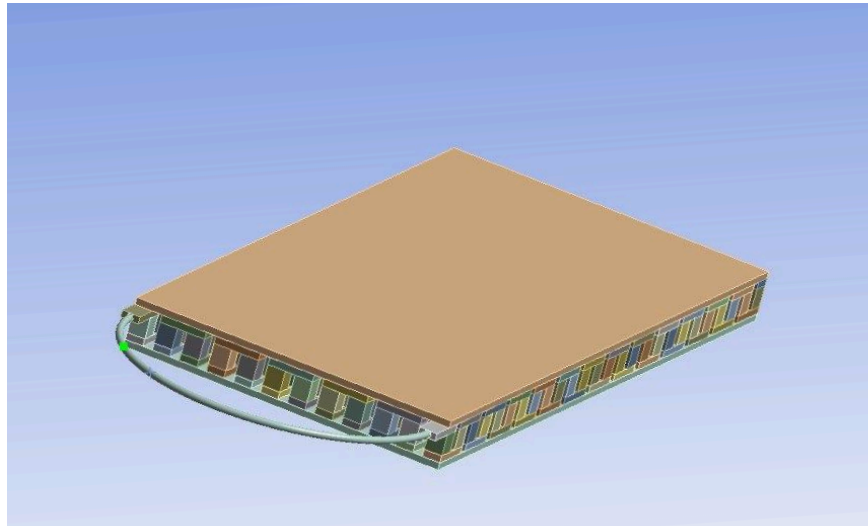


*Figure 9. Simplified TEG module for simulation*

### **3.3 Braking energy dissipation**

Toyota Camry was chosen as a test vehicle and the specifications are as follows: a mass of 1467 kilograms, an initial speed of 40, 60 and 80 kilometers per hour [10]. The car specification data states that the stopping distance of the vehicle is 45 meters at 60 kilometers per hour. These numbers contribute to the finding friction factor of the vehicle with the road and

stopping distance at other initial velocities. The braking efficiency distribution will be 30% on the one front wheel ( $\lambda = 0.3$ ) [1].

$$E_L = KE = \frac{1}{2}m\vartheta^2 \quad (3)$$

$$a = \frac{\vartheta_f^2 - \vartheta_0^2}{2(x_f - x_0)} \quad (4)$$

$$t = \frac{v_0}{a} \quad (5)$$

$$s = \frac{\vartheta_0^2 - \vartheta_f^2}{2gf} \quad (6)$$

$$P_{front\ wheel} = \frac{E_L}{t} \times \lambda \quad (7)$$

$$A_{disk} = \frac{\pi(d_{outer}^2 - d_{inner}^2)}{4} \quad (8)$$

$$q = \frac{P_{front\ wheel}}{A_{disk}} \quad (9)$$

where  $E_L$  is energy loss,  $KE$  is kinetic energy,  $m$  is mass of car,  $\vartheta_f$  is final speed,  $\vartheta_0$  is initial speed,  $x_f$  is final distance,  $x_0$  is initial distance,  $a$  is deceleration,  $s$  is stopping distance of vehicle,  $g$  is acceleration due to gravity,  $f$  is friction factor,  $t$  is braking time,  $P_{front\ wheel}$  is braking power,  $\lambda$  is braking efficiency distribution,  $q$  is heat flux and  $A_{disk}$  is the braking section area.

Using Formulas from 3 to 9, total energy losses, heat fluxes can be derived for one front wheel. The braking section area equals  $0.0368\ m^2$ .

Table 4. Braking power and heat flux for different scenarios

Parameter	Unit	Scenario 1	Scenario 2	Scenario 3
$\vartheta_0$	km/h	40	60	80
$\vartheta_0$	m/s	11.11	16.67	22.22
$t$	s	3.6	5.4	7.2
$s$	m	19.99	45.00	79.97
$P_{front\ wheel}$	W	7548.39	11319.45	15096.79
$q$	W/m <sup>2</sup>	205 308.74	307 877.56	410 617.47

It can be stated that a large amount of energy can be recovered during the braking of a vehicle, where most of the energy dissipates in the form of heat to the environment.

### 3.4. Thermal analysis by ANSYS simulations

To obtain the temperature difference for the TEG simulations and calculations of the output voltage and power, we conducted a thermal analysis of the braking rotor during the braking process. For this purpose, the selected methodology was running the simulations in ANSYS transient thermal. The thermal distribution of the brake rotor is needed to choose the best spot for fastening the thermoelectric generators, as well as provide the necessary calculations to estimate the output values.

First step for the simulation execution: import of the CAD files into ANSYS' working directory. We used the STEP format for that task. After this the meshing has to be done. In our case, tetrahedral mesh was used, and the mesh sizing on the surfaces that will be analyzed were significantly increased. This allows more accurate results for the simulations.

The total number of the elements happened to be 1605466.

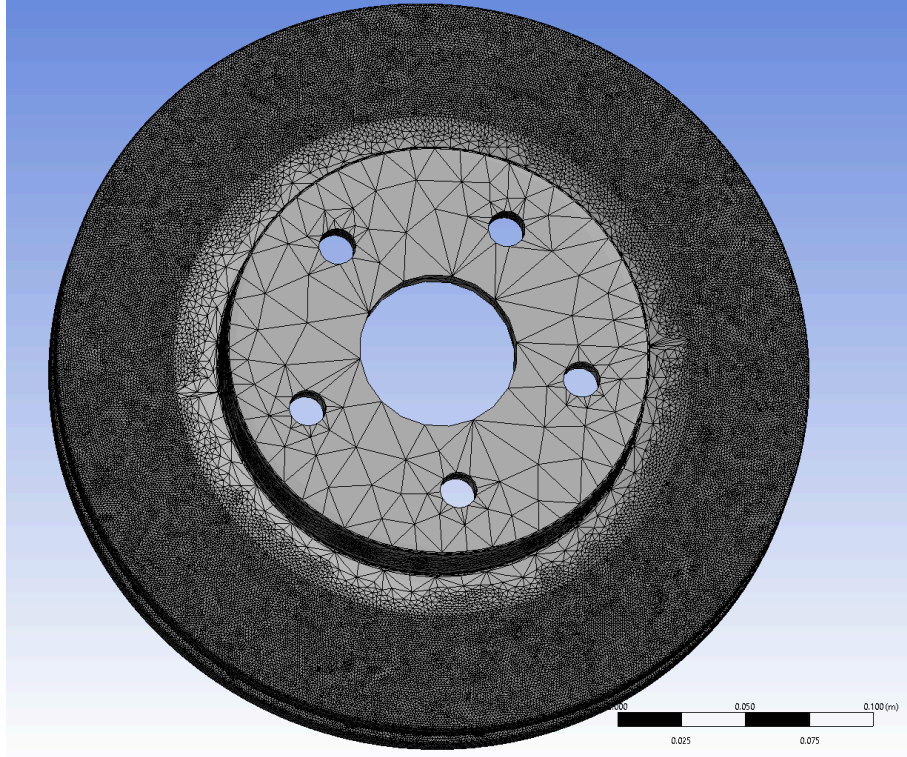


*Figure 10. Meshing of brake disk*

After the mesh is completed, the boundary conditions need to be set. In order to simulate heat generation due to friction in a braking disk, we set the heat flux to the planes that will be in contact with the brake pads. We are considering a ventilated disk, so the convection should also be considered as a factor.

As a result, we get a temperature distribution contour, to find the hottest region of the inner part of the rotor. The temperature that will be illustrated there will then be used in order to calculate and simulate the output power and output voltage.

### **3.5. TEG analysis by ANSYS simulations**

Firstly, the same approach for meshing, was used to create the mesh for the thermoelectric generator:



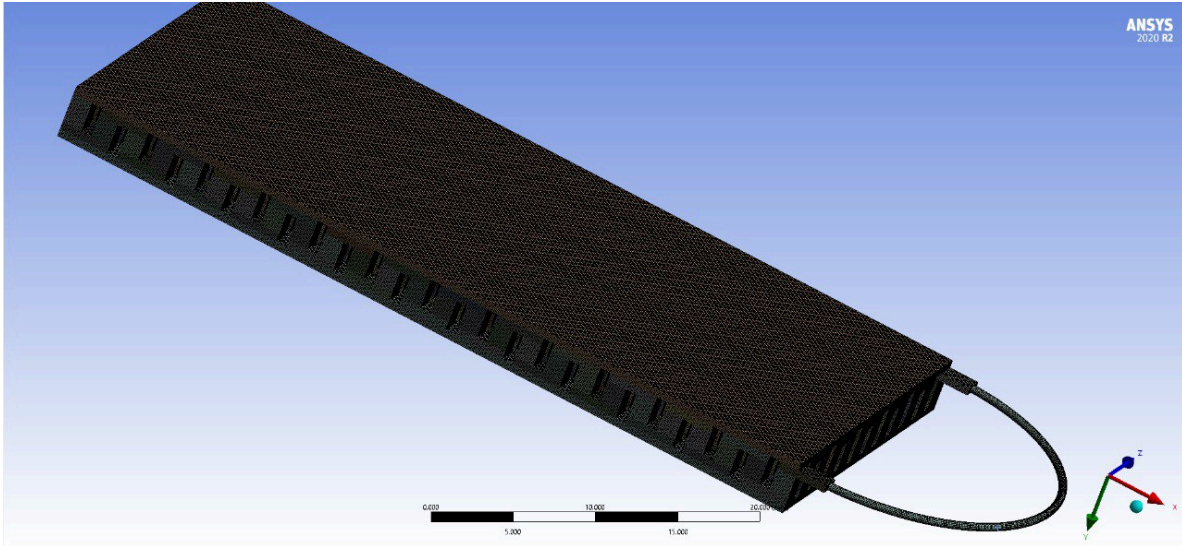


*Figure 11. Mesh for the TEG*

For the analysis, the thermal electric conduction steady state was used to simulate the power generation of the TEG.

The input boundary conditions are hot side temperature, cold side temperature and a wire convection.

## **4. RESULTS AND DISCUSSION**

### **4.1. Ansys results**

#### **4.1.1 Thermal analysis of a rotor.**

ANSYS simulations results for the temperature distribution for braking from different velocities are represented in the figures below:

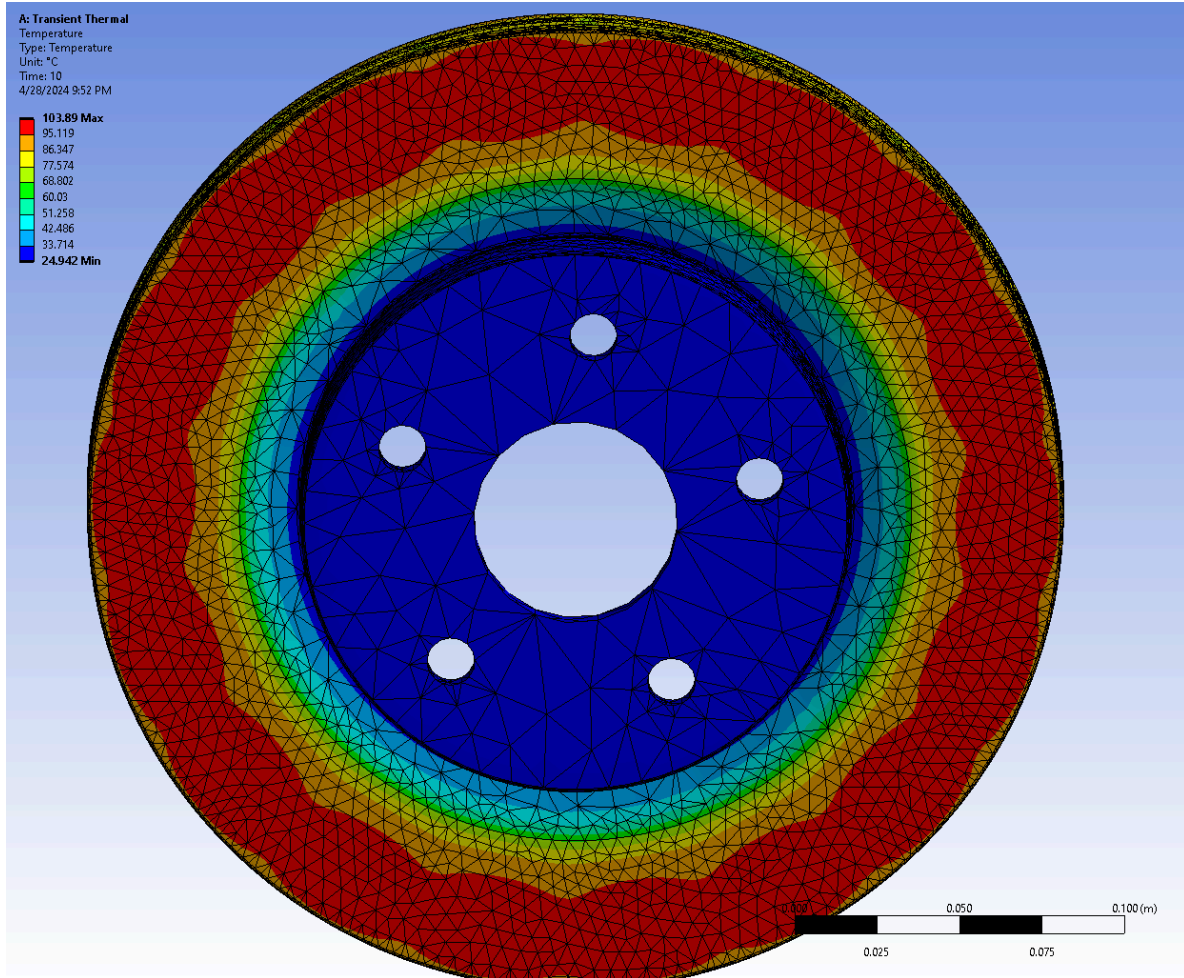


*Figure 12. Front side temperature distribution for 40km/h*

From the figure 12 that illustrates the temperature distribution for the part of the disk that is in contact with the brake pads for the process of braking from 40 km/h, we can note that the disk during that braking is heated to the maximum temperature of nearly 104 degrees Celsius. The value of heat flux was taken from the MATLAB calculations described in the passage prior to that. The convection coefficient is taken from the Scientific paper (Belhocine, A. 2017) [11].

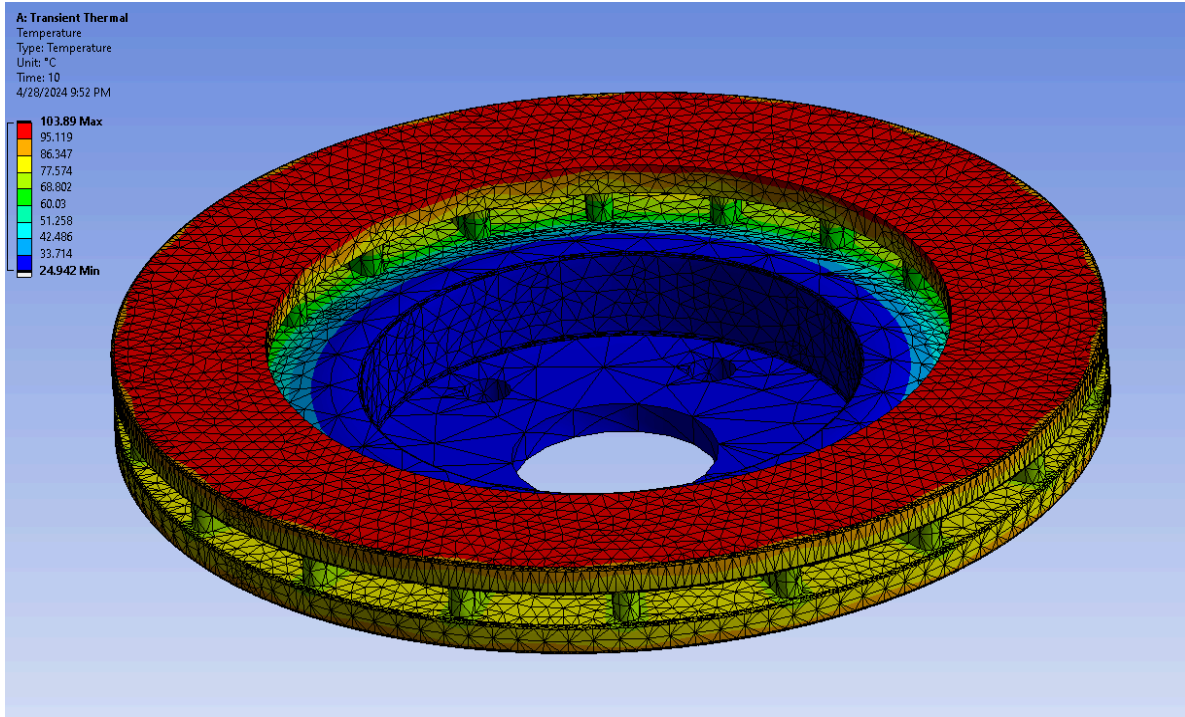


*Figure 13. Back side temperature distribution for braking from 40 km/h*

What is crucial data for the further analysis is the temperature on the inner surface of the brake disk. For our calculations we used 10s as a braking time for each velocity varying the heat flux. For 40 km/h, the inner surface of the disk heated to the temperature maximum of 86.25 degrees Celsius in 10 s, as illustrated in figure 13. The initial temperature of both surfaces is 25 degrees Celsius and decided to do the analysis for only 1 braking cycle. The more times a vehicle performs braking, the higher the initial temperature is going to be for the next braking, so during urban use, the temperature can be much higher which will positively affect the performance of the TEG.

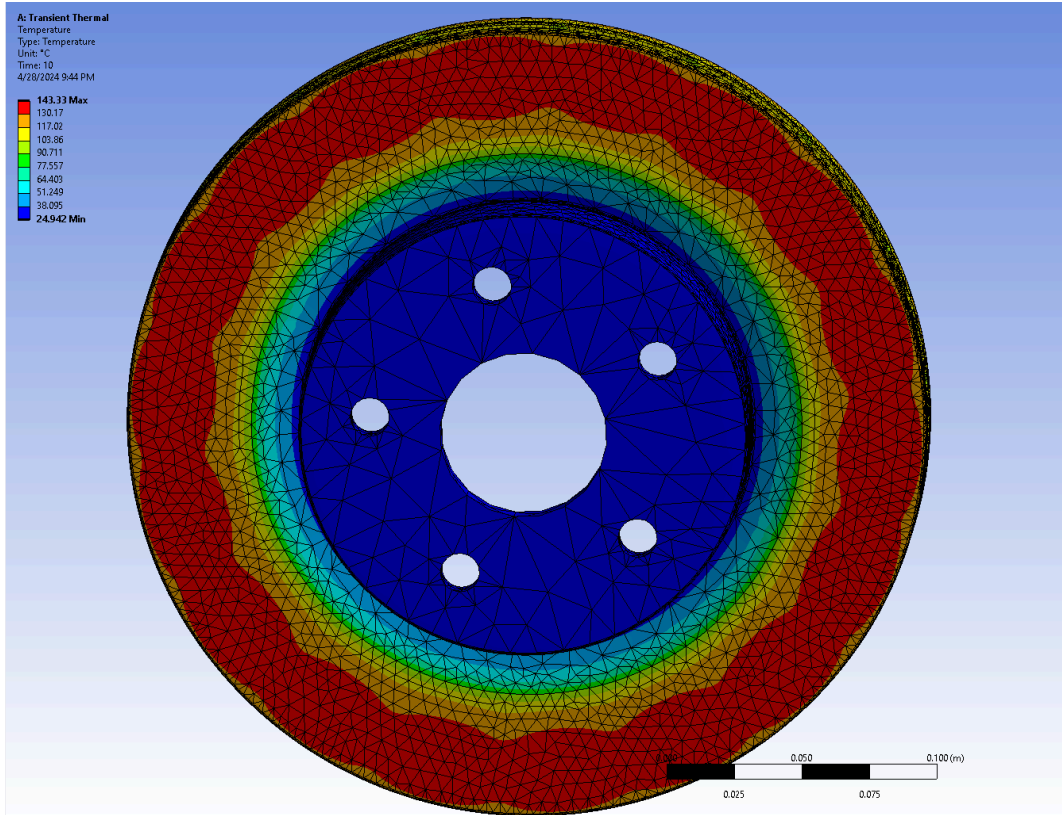


*Figure 14. Front side temperature distribution for braking from 60 km/h*

Here in figure 14, it can be seen that the maximum temperature for the braking disk that stops from 60 km/h, is 143 degrees Celsius. This is the regular speed limit for vehicles in cities in the majority of the world. This speed, as can be seen in the contour, can already produce a sufficient amount of dissipated heat energy from one braking cycle.

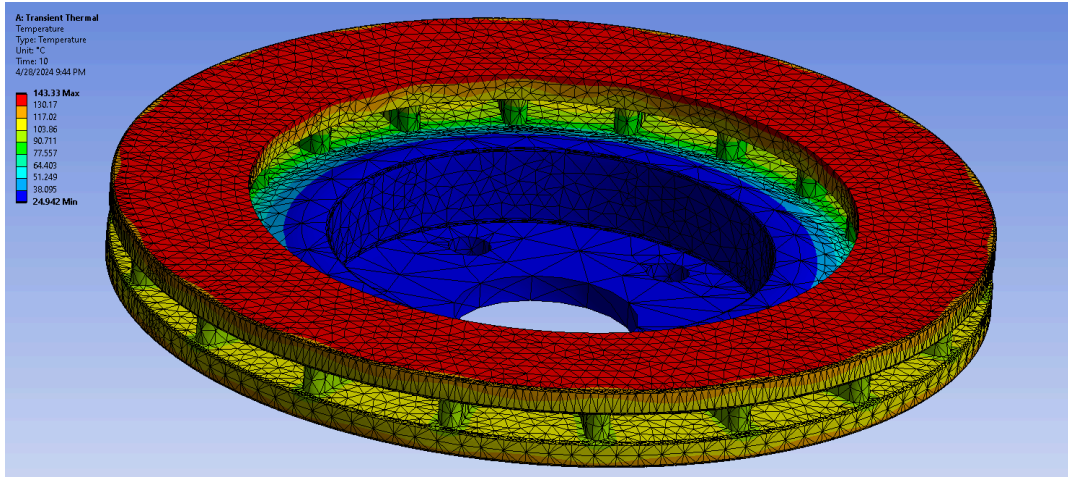


*Figure 15. Back side temperature distribution for braking from 60 km/h*

For the inner side of the rotor, the temperature of the surface reaches 117 degrees Celsius. This is a temperature that already can give us a sufficient power output for our system in one braking cycle. Results are illustrated in figure 15.

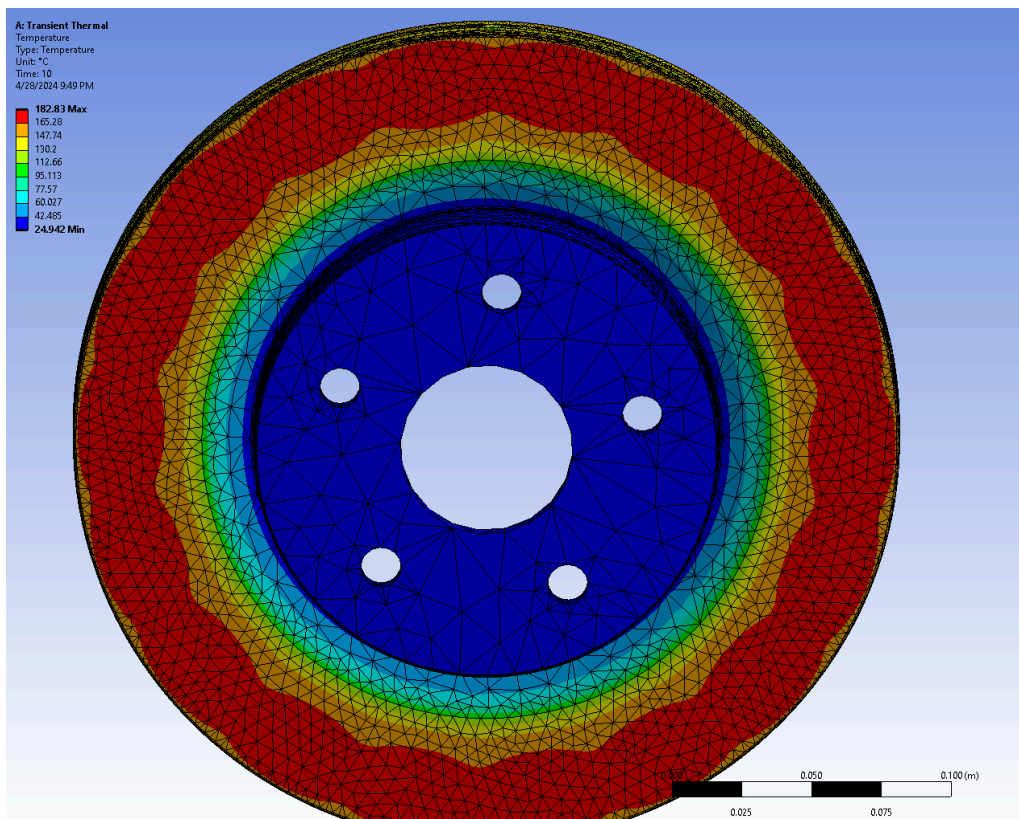


*Figure 16. Front side temperature distribution for braking from 80 km/h*

Now for the last braking cycle we decided to check the braking from 80 km/h. Here in figure 16, it can be seen that the brake disk can reach the temperature up to 182 degrees Celsius, which is a very sufficient temperature for the operation of the system.

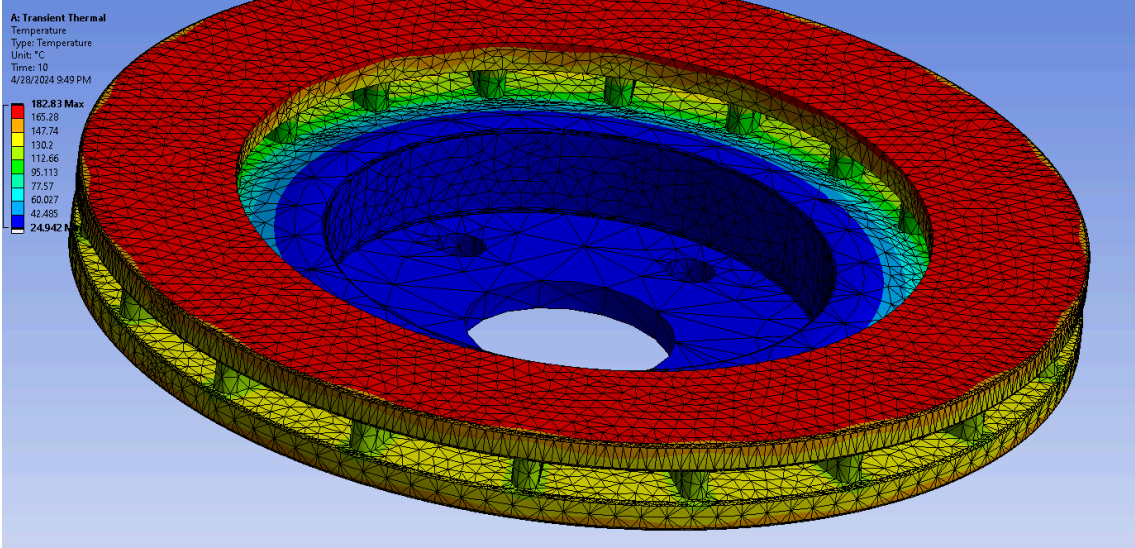


Figure 17. Back side temperature distribution for braking from 80 km/h

Figure 17 illustrates the temperature distribution on the inner side of the brake disk for the braking cycle from 80 km/h. The output temperature that TEG will use after one 10s braking cycle is 147 degrees Celsius.

### 4.1.2 TEG Analysis

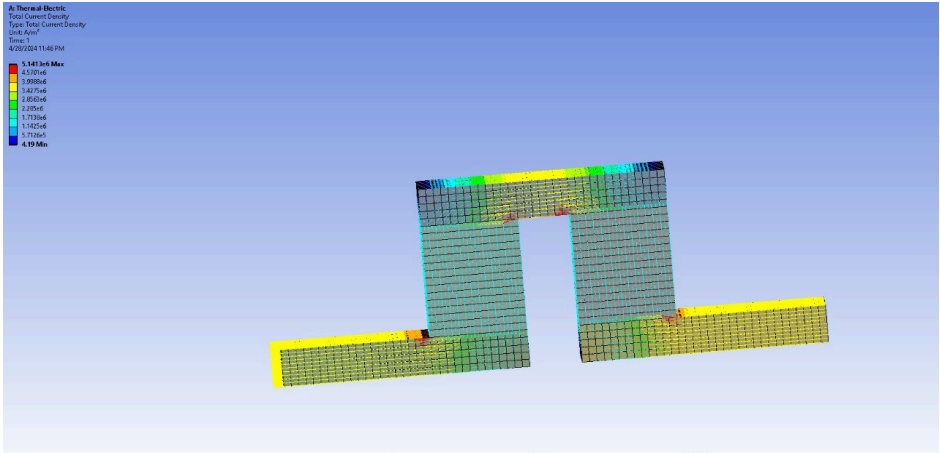


Figure 18. Results for the total current density.

Figure 18 illustrates the results for the current density for a single N-P type pair. The current is sufficient considering it is a single element.

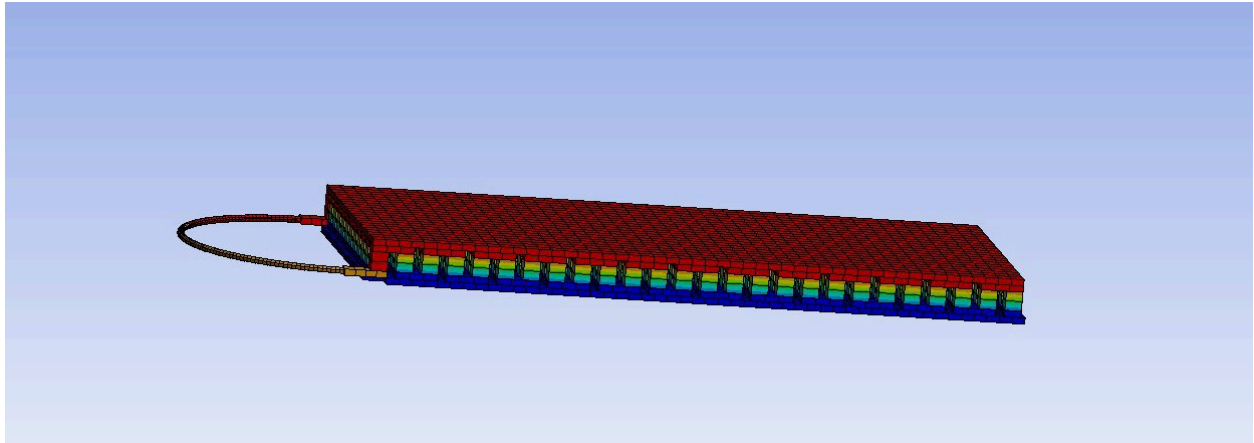


Figure 19. Thermal analysis of a TEG.

Figure 9 Illustrates the temperature distribution along the TEG. It can be seen that the distribution is exactly how it is supposed to be with a clear hot and cold sides.

Overall, the result of output power generated was calculated by multiplication of power density on volume. The output power for 40 km/h is 0.529 W, for 60 km/h is 1.272 W and for 80 km/h is 2.066 W.

#### 4.2. The TEG module's parameters calculations

Table 6. Maximum parameters of single TEG at different temperatures

Parameter	Unit	1	2	3
$\vartheta_0$	km/h	40	60	80
$T_h$	°C	86.37	117.05	147.79
$T_c$	°C	25	25	25
$I_{max}$	A	0.833	1.250	1.667

$V_{max}$	$V$	3.934	5.900	7.871
$W_{max}$	$W$	0.819	1.843	3.280
$\eta_{max}$	%	1.966	2.909	3.828
$\eta_{mp}$	%	2.650	3.588	4.353

It is clearly observed that higher temperature at hot junctions leads to the better performance of the TEG module. For instance, single TEG module produces 3.280 W at 147.79 °C, which is 4 times larger than module which generates a temperature of 86.37 °C. In comparison with other works, the TEG of Coulibaly et al. (2021) produced 3.25 W for ventilated brake disk of power at 175.92 °C, but they did not clearly show the location of the TEG module in the braking system.

Comparing the results of the simulations with the calculations, a considerable difference can be observed. The error distribution among 40 km/h, 60 km/h, and 80 km/h distributes at approximately 35%. It is a considerable uncertainty, however both results are within the satisfactory range. The difference in the obtained results happened because of the different methodology that was applied for the problem solving, as well as the absence of wire insulation in the simulations set up. ANSYS workbench provides us with the perfect conditions which are different from real world situations, which resulted in increased error.

Figures below show the relationship of thermal efficiency, electrical current, voltage across the module and power output with external load resistance for different temperatures at hot junctions.



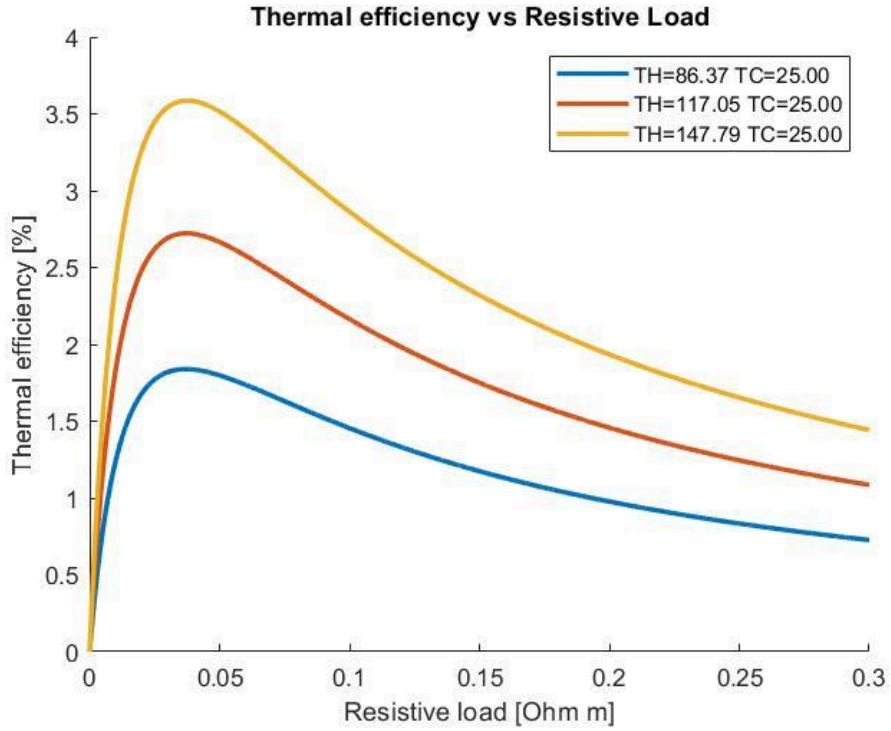


Figure 20. Thermal efficiency against resistive load graph

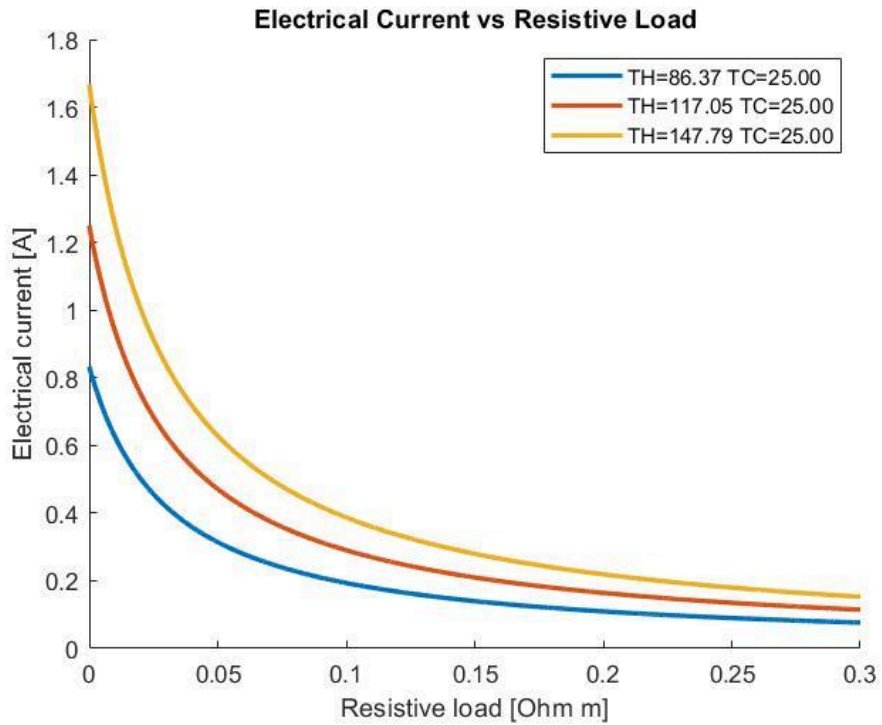


Figure 21. Electrical current against resistive load graph

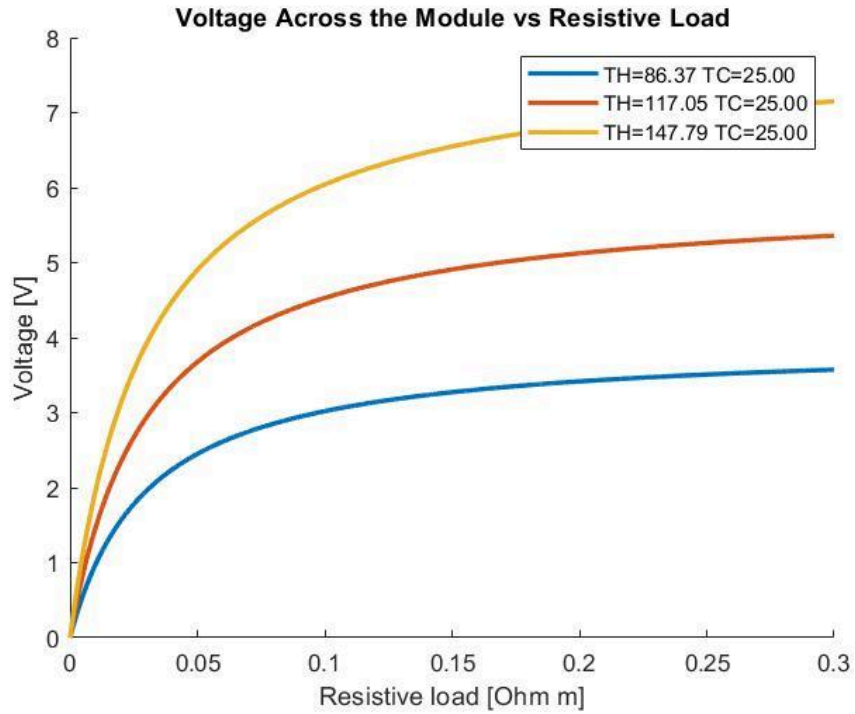


Figure 22. Voltage against resistive load graph

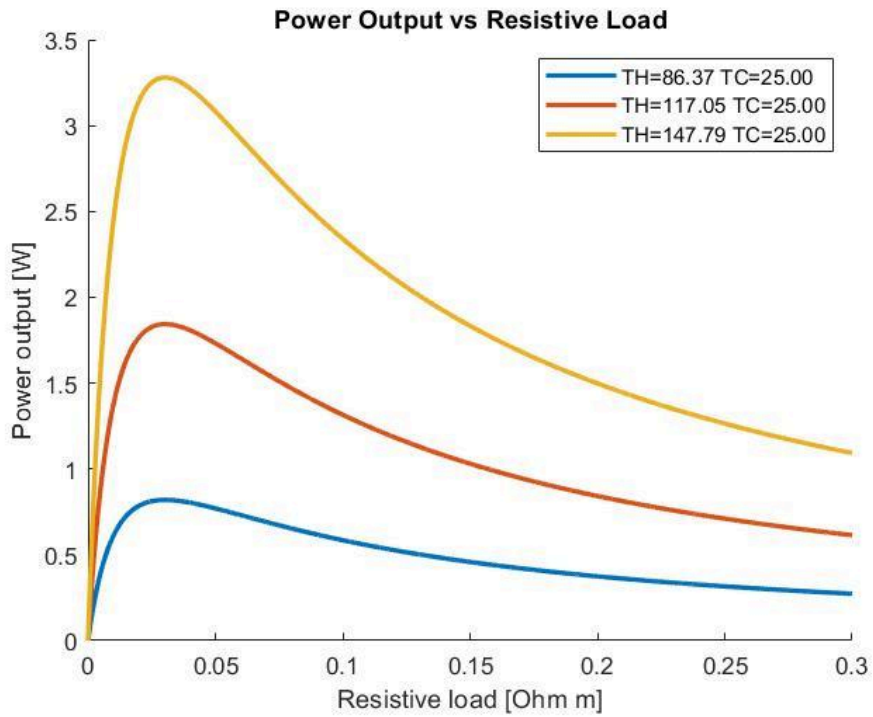


Figure 23. Power output against resistive load graph

The number of TEG modules inside the brake disk is 9 and they are connected in series. Therefore, the power outputs of all modules are 7.37 W for 40 km/h, 16.59 W for 60 km/h and 29.52 W for 80 km/h, respectively. According to Coulibaly et al. (2021), their generated power output of 3.25 W and 4.25 W for full and ventilated disk is applicable to power the on-board instrumentation. Therefore, TEG's power output is enough to power an electrical system in our proposed case.

### **4.3. Our team's proposed design**

This section provides a full design of TEGs integrated with other parts of the car. This design was made based on the analysis of available areas of displacement of the TEGs. In addition, a serious problem was connected with wiring. As our TEGs are located on a rotating element, the problem of wiring from a rotating part to a fixed part of the car had to be solved. A conceptual solution of the wiring problem was first shown by Jie (2015). He suggested using the conductive ring, a device which allows the transmission of electricity between rotating and fixed parts.

The TEGs (1) are connected in series by wires (2) and the design can be shown in Figure 24. There are input and output wires which are connected to the rotor (4). The stator (3) is mounted on the wheel hub (5) which is a stationary part of the car.

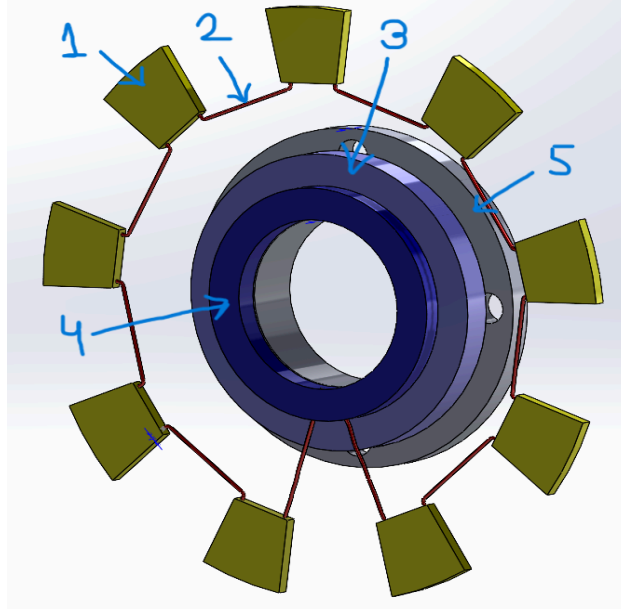


*Figure 24. The design of the TEGs connection with the slip ring with wirings*

The coating of the wiring requires attention as they are in a harsh environment in terms of high temperature, vibration and dynamic force. These conditions require such characteristics from protection material such as high temperature resistance, relatively high strength, flexibility and corrosion resistance. The braided cable shield is an appropriate solution to this problem. This type of wire protection meets all the requirements.

The next problem we faced was placement of the slip ring. There is not much space in the car's wheel sector. However, the space between the disk and wheel hub allows the slip ring to be placed there. The rotor of the slip ring is mounted on the rotating part of the wheel hub (6), while the stator is fixed on the stationary part of the wheel hub (7).

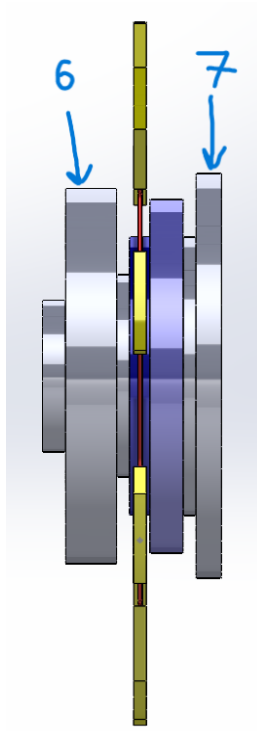


Figure 25. Side view of the TEGs connection with the slip ring with wirings

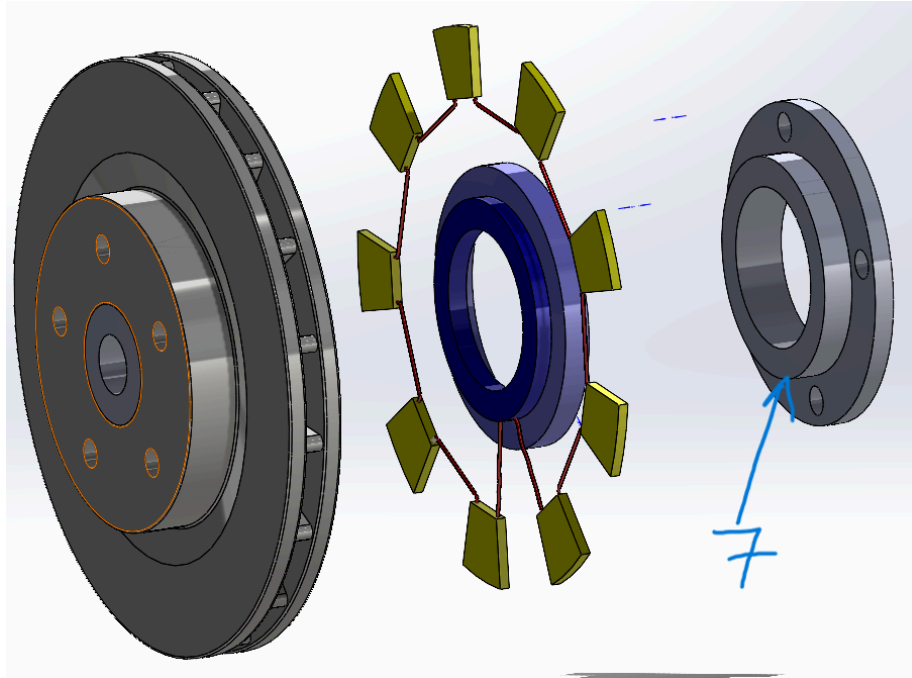


Figure 26. Exploded view of the TEGs connection with the slip ring with wirings

## 5. CONCLUSION

As a result of the study, the performance of the TEG was explored and the optimal design for the TEG set up was proposed. Overall, most of the energy that is dissipated in the brake disk remains lost. However, even with the low efficiency the amount of energy that was recuperated from the rotor is still sufficient to implement a helpful electrical system.

The recharging of the battery can significantly reduce the fuel consumption for any vehicle, since there is no need for the engine to continuously operate when the vehicle is at rest, which also is an economical benefit for their users.

For a single break cycle, the study has shown that the amount of energy that 9 thermoelectric generators can recuperate is sufficient for an urban operation. For a low speed limit of 40 km/h, the generated power for a single brake cycle came out to be 7.37 W. Even though it is a relatively small number, it can serve as a good support for electric systems in any vehicle.

For faster speed limits of 60 km/h and 80 km/h, the respective power outputs turned out to be 16.59 W and 29.52 W. This power, however, is enough for more advanced applications such as control systems, navigation devices, battery charging etc.

## REFERENCES

- [1] Coulibaly, A., Zioui, N., Bentouba, S., Kélouwani, S., & Bourouis, M. (2021). Use of thermoelectric generators to harvest energy from motor vehicle brake discs. *Case Studies in Thermal Engineering*, 28, 101379. <https://doi.org/10.1016/j.csite.2021.101379>
- [2] Lee, H. S. (2016). Thermoelectrics: design and materials. In *Wiley eBooks*. <https://doi.org/10.1002/9781118848944>
- [3] Dziurdzia, P. (2011). Modeling and simulation of thermoelectric energy harvesting processes. In *InTech eBooks*. <https://doi.org/10.5772/28530>
- [4] SR012 Low Voltage Slip Ring Separates by Rotary Systems, Inc. (2022, June 29). Rotary Systems. <https://rotarysystems.com/slip-rings/product/3-amps-to-210-vdc-separates/>
- [5] Grandin, M., & Wiklund, U. (2016). Wear and electrical performance of a slip-ring system with silver–graphite in continuous sliding against PVD coated wires. *Wear*, 348–349, 138–147. <https://doi.org/10.1016/j.wear.2015.12.002>
- [6] Zhang, J. (2015). Design of automobile brake waste heat recovery device. *Advances in Engineering Research/Advances in Engineering Research*. <https://doi.org/10.2991/asei-15.2015.387>
- [7] *Disk brake Toyota Camry*. (n.d.). Walmart. <https://www.walmart.com/ip/C-Tek-Disc-Brake-Rotor-121-44146-Fits-select-2006-2018-TOYOTA-RAV4-2007-2017-TOYOTA-CAMRY/34260556>
- [8] Kumar, B. B. (2021). Thermal analysis of disc brake rotor. *IJERT*. <https://doi.org/10.17577/IJERTV10IS050301>

- [9] Lv, H., Li, G., Zheng, Y., Jiagen, H., & Li, J. (2018). Compact Water-Cooled Thermoelectric Generator (TEG) based on a portable gas stove. *Energies*, *11*(9), 2231.  
<https://doi.org/10.3390/en11092231>
- [10] *2017 Toyota Camry LE Price & Specifications - The Car Guide*. (n.d.). The Car Guide.  
<https://mobile.guideautoweb.com/en/specifications/toyota/camry/le/2017/>
- [11] Belhocine, A., & Wan-Omar, W. Z. (2017). CFD modeling and computation of convective heat coefficient transfer of automotive disc brake rotors. *Revista científica*, (29), 116-128.  
<https://revistas.udistrital.edu.co/index.php/revcie/article/view/11602/15003>
- [12] Skomedal, G. (2016). *Thermal durability of novel thermoelectric materials for waste heat recovery*. <http://hdl.handle.net/11250/2391043>



## APPENDICES

### Code 1. Calculation and graphical representation of TEG power output

```
thermalconP = 1.68; % W*m^-1*K^-1
thermalconN = 1.64; % thermal conductivity

resisP = 1.83*10^-5; % Ohm*m
resisN = 1.58*10^-5; % electrical resistance

SeebeckP = 223.2*10^-6; % V/K
SeebeckN = -187.7*10^-6; % Seebeck coefficient

L = 0.0015; % Leg length
A = 1.3*1.3*10^-6; % Cross-sectional area of Leg

increment = 0.0001; % resistive load increment
resistive_load_values = 0:increment:0.3; % resistive Load Ohm

n = 156; % number of thermocouples

% Prompt the user to input values for two variables
TH_str = input('Enter the value for TH (separated by spaces): ',
's');
TC_str = input('Enter the value for TC (separated by spaces): ',
's');

% Convert the string inputs to numeric arrays
TH = str2num(TH_str);
TC = str2num(TC_str);

SeebeckOut = SeebeckP - SeebeckN;
InRes = (resisP * L/A) + (resisN * L/A); % internal resistance
TherCon = thermalconP * A/L + thermalconN * A/L; % thermal
conductance
Z = SeebeckP^2/(thermalconP*resisP);

for i = 1:length(TH)
    Imax = SeebeckOut*(TH(i) - TC(i))/InRes;
    Vmax = n*SeebeckOut*(TH(i) - TC(i));
```

```

    Wmax = (n*SeebeckOut^2*(TH(i) - TC(i))^2)/(4*InRes);
    nmp = 100 *
    (((1-(TC(i)+273.15)/(TH(i)+273.15))./(2-0.5*(1-(TC(i)+273.15)/(TH(i)+2
73.15))+2/(Z*0.5*(TC(i)+273.15)*(1+(TC(i)+273.15)/(TH(i)+273.15))))));
    nmax = 100 * (1 - (TC(i)+273.15)/(TH(i)+273.15)) * ((-1 + (1 +
Z*0.5*(TC(i)+TH(i)+273.15+273.15))^0.5) /
((TC(i)+273.15)/(TH(i)+273.15) + (1 +
Z*0.5*(TH(i)+TC(i)+273.15+273.15))^0.5));
    fprintf('For TH = %f and TC = %f:\n', TH(i), TC(i));
    fprintf('Imax: %f\n', Imax);
    fprintf('Vmax: %f\n', Vmax);
    fprintf('Wmax: %f\n', Wmax);
    fprintf('nmax (maximum convection (thermal) efficiency): %f\n',
nmax);
    fprintf('nmp (maximum power efficiency): %f\n', nmp);
end

figure;
hold on

for i = 1:length(TH)
    I(i, :) = SeebeckOut * (TH(i) - TC(i))./(InRes +
resistive_load_values); % electrical current for the module
    Vn(i, :) = n * SeebeckOut * (TH(i) -
TC(i)).*(resistive_load_values/InRes)./(resistive_load_values/InRes +
1); % voltage across the module
    Wn(i, :) = n * SeebeckOut^2 * (TH(i) - TC(i))^2 .*
(resistive_load_values/InRes)./(InRes * (1 +
resistive_load_values/InRes).^2);
    Qh(i, :) = n * (SeebeckOut*(TH(i) + 273.15) .* I(i, :) - 0.5 .*
I(i, :).^2 * InRes + TherCon * (TH(i) - TC(i)));
    nth(i, :) = 100*Wn(i, :)./Qh(i, :);
    % Plot the power output for each combination of TH and TC
    plot(resistive_load_values, Wn(i, :), 'LineWidth', 2);
end

xlabel('Resistive load [Ohm m]');
ylabel('Power output [W]');
title('Power Output vs Resistive Load');

```

```

legend(cellstr(num2str([TH', TC'], 'TH=%-3.2f TC=%-3.2f')));

figure;
hold on

for i = 1:length(TH)
    plot(resistive_load_values, I(i, :), 'LineWidth', 2);
end

xlabel('Resistive load [Ohm m]');
ylabel('Electrical current [A]');
title('Electrical Current vs Resistive Load');
legend(cellstr(num2str([TH', TC'], 'TH=%-3.2f TC=%-3.2f')));

figure;
hold on

for i = 1:length(TH)
    plot(resistive_load_values, Vn(i, :), 'LineWidth', 2);
end

xlabel('Resistive load [Ohm m]');
ylabel('Voltage [V]');
title('Voltage Across the Module vs Resistive Load');
legend(cellstr(num2str([TH', TC'], 'TH=%-3.2f TC=%-3.2f')));

figure;
hold on

for i = 1:length(TH)
    plot(resistive_load_values, nth(i, :), 'LineWidth', 2);
end

xlabel('Resistive load [Ohm m]');
ylabel('Thermal efficiency [%]');
title('Thermal efficiency vs Resistive Load');
legend(cellstr(num2str([TH', TC'], 'TH=%-3.2f TC=%-3.2f')));

```